Evolutionary Ecology Research, 2007, **9**: 675–695

Niche expansion: coupled evolutionary branching of niche position and width

Hiroshi C. Ito* and Masakazu Shimada

Graduate School of Arts and Sciences, University of Tokyo, 3-8-1 Komaba, Meguroku, Tokyo 153-8902, Japan

ABSTRACT

Question: Does evolutionary niche expansion of a consumer population from its original resource to a new resource induce coupled evolutionary branching of niche position and width?

Key assumption: The position and width of an individual resource utilization pattern (niche) are evolutionary traits, which form a two-dimensional phenotype space. The resource distribution is bimodal.

Methods: The possibility of evolutionary branching through resource competition was examined with adaptive dynamics theory, i.e. an extension of ESS theory. Evolutionary dynamics was also simulated using an individual-based model with sexual reproduction.

Conclusion: Diversification in niche position only is suppressed by directional evolution of niche width. Nevertheless, evolutionary branching occurs almost always in this model, and involves joint diversification of niche width and niche position. When specialist strategies that initially utilize only one resource undergo evolutionary branching, the incipient branches differ strongly in niche width. Eventually, the branch with the larger niche width will develop into a specialist utilizing the new resource.

Keywords: adaptive dynamics, evolutionary branching, niche width, resource competition, resource utilization pattern.

INTRODUCTION

Resource competition is important for understanding how present biological communities have developed through their evolutionary history. Various organisms consume various kinds of resources in various ways. The form of resource use (i.e. the distribution of utilization intensities for resources) is termed the utilization pattern or niche. Variations among niches have been investigated with two main measures: niche position and niche width (Pianka, 1983). Niche position corresponds to the main resource that is fed on, while niche width corresponds to the variety of resources that can be fed on. Suppose that resources are sorted along an axis of a resource property (such as size, hardness or nutrient composition), so that focused niches are represented as unimodal distributions. Then, an

* Author to whom all correspondence should be addressed. e-mail: itoh9@dolphin.c.u-tokyo.ac.jp
Consult the copyright statement on the inside front cover for non-commercial copying policies.

© 2007 Hiroshi C. Ito

organism with a narrow niche corresponds to a specialist with a limited variety of food, whereas one with a wide niche corresponds to a generalist with a wide variety of food.

Organisms show large variations not only in their niche position but also in their niche width. From the perspective that those organisms are derived from a universal ancestor (Di-Giulio, 2001), both niche position and niche width should be important evolutionary components that have experienced significant diversification with repeated evolutionary branching. Moreover, the evolution of niche position and width should be correlated, because the widening of the average niche width of a population has similar effects to diversification of its niche position through evolutionary branching, at the level of species group (Pianka, 1983; Ackermann and Doebeli, 2004). Thus evolutionary branching by coupled diversification of niche position and width might have occurred.

While most theoretical studies have focused on the evolutionary branching of niche position only (Metz *et al.*, 1996; Meszena *et al.*, 1997; Geritz *et al.*, 1998; Dieckmann and Doebeli, 1999; Doebeli and Dieckmann, 2000), two recent papers examined evolutionary branching of asexual populations using both niche position and width as evolutionary traits (Ackermann and Doebeli, 2004; Egas *et al.*, 2005), extending the MacArthur-Levins competition model (MacArthur, 1972). In the model of Ackermann and Doebeli (2004), evolutionary branching occurs only in niche position. In contrast, Egas *et al.* (2005) showed numerically evolutionary branching that involves diversification of niche width as well as position, but what circumstances allow such branching are unclear.

In this study, we investigate the conditions and mechanism for the coupled evolutionary branching of niche position and width, using both analytical and numerical approaches. In particular, we focus on bimodal resource distributions (i.e. two kinds of resources). This is because the evolution of niche width can have a critical role during niche expansions from an original resource to a new one, for utilization of the new and original resources simultaneously, and for specialization to the new resource. Evolutionary branching involving diversification of niche width might be favoured by selection in such a situation.

Based on adaptive dynamics theory (Dieckmann and Law, 1996; Metz *et al.*, 1996; Geritz *et al.*, 1997), we analyse the possibility for and characteristics of evolutionary branching when there are differences in the quality and quantity of the two resources. To test the predictions of this analysis, we also simulate the evolutionary dynamics in an individual-based stochastic model with sexual reproduction.

THE MODEL

We assume that resources are organisms. Although a resource–consumer (predator–prey) interaction generally induces the co-evolution of consumers and resources, the evolution of resources is not considered here, since our interest is the evolutionary reaction of a consumer population to a bimodal resource distribution. Specifically, we assume two species for the resources (prey), and a two-dimensional phenotype space $x = (\mu, \sigma)$ for the consumers (predators). The traits μ and σ determine the position and width of individual utilization pattern, respectively. We describe their population dynamics by

$$\frac{dn(x)}{dt} = c \cdot n(x)[g_1(x) + g_2(x)] - d \cdot n(x), \tag{1}$$

$$\frac{dR_1}{dt} = \gamma \cdot R_1 \left[1 - \frac{R_1}{K_1} \right] - \int n(x) \cdot g_1(x) dx, \tag{2}$$

$$\frac{dR_2}{dt} = \gamma \cdot R_2 \left[1 - \frac{R_2}{K_2} \right] - \int n(x) \cdot g_2(x) dx, \tag{3}$$

where $n(x)$, R_1, and R_2 denote the biomass of predator phenotype x and that of the two prey species 1 and 2, respectively. The biomasses of prey grow with a constant intrinsic growth rate, γ, under phenotype-specific carrying capacities, K_1 and K_2. The second terms in equations (2) and (3) are their biomass losses by predation. $g_1(x)$ and $g_2(x)$ are functional responses (i.e. predation rates by unit biomass of predator) of predator phenotype x to prey 1 and 2, respectively. In equation (1), each phenotype x increases its biomass by its predation amount multiplied by a constant trophic efficiency c, and decreases its biomass by a constant natural death rate d.

It is ecologically plausible that the functional response depends both on the property of the resource and on the utilization intensity of the consumer. To express this dependency explicitly, we introduce an axis of resource property z, on which the prey are represented as resources. Since differences in developmental stages and in nutritional conditions would make certain variation as a resource in each of the prey species, we define the resource distribution provided by unit biomass of species i (= 1 or 2), with a Gaussian distribution,

$$r_i(z) = \frac{1}{\sqrt{2\pi}\sigma_R} \exp\left(-\frac{(z - y_i)^2}{2\sigma_R^2} \right), \tag{4}$$

where the centre and width (standard deviation) of the distribution are determined by y_i and a constant σ_R, respectively. Summing the two resources gives the total resource distribution:

$$R(z) = R_1 \cdot r_1(z) + R_2 \cdot r_2(z). \tag{5}$$

On the other hand, we treat the utilization pattern of predator phenotype $x = (\mu, \sigma)$ as a frequency distribution of utilization intensity, and define it by

$$u(z, x) = \frac{1}{\sqrt{2\pi}\sigma} \exp\left(-\frac{(z - \mu)^2}{2\sigma^2} \right). \tag{6}$$

The total utilization distribution is given by

$$U(z) = M \int n(x) u(z, x) dx, \tag{7}$$

where the constant M denotes the amount of utilization provided by unit biomass of the predator.

Functional responses generally depend on the densities of both prey and predators (Abrams and Ginzburg, 2000). To express this without loss of simplicity, we assume the following. First, predators recognize resources only by their property z. Second, the predation rate on any resource per unit utilization density is an identical function among all kinds of predators, which is given by

$$H(z) = \Omega \cdot \frac{R(z)}{\beta + \beta' \cdot U(z) + R(z)}. \tag{8}$$

This function corresponds to a general form of functional response, the *Beddington-DeAngelis* type (Beddington, 1975; DeAngelis *et al.*, 1975). As $R(z)$ increases, the response increases but does not exceed Ω, which corresponds to saturation of predation. On the other hand, as $U(z)$ increases, the response decreases, which corresponds to interference competition

among predators. [$\beta = 0$ gives the *ratio-dependent* response (Arditi and Ginzburg, 1989), while $\beta' = 0$ gives the Holling type-II response.]

The response of phenotype x to resource z is given by $Mu(z, x)\,H(z)$, and the fraction of resource i in resource z is $R_i r_i(z)/R(z)$. Then the functional response of phenotype x to resource i is given by

$$g_i(x) = \int Mu(z, x)\,H(z) \cdot \frac{R_i r_i(z)}{R(z)}\,dz, \tag{9}$$

based on the first assumption above. Substitution of this equation into equations (1)–(3) gives the full population dynamics of the predator–prey (consumer–resource) system. Note that equation (1) can be transformed into

$$\frac{dn(x)}{dt} = n(x)\left[cM\int u(z,x)\cdot H(z)dz - d\right]. \tag{10}$$

For efficiency of investigation, we introduce an additional three parameters: D_R, the magnitude of the difference between the resources; A_R, the asymmetry in biomass between the resources; and R_0, the magnitude of the resource distribution. Then, y_1, y_2, K_1, and K_2 are given by

$$(y_1, y_2) = \left(\frac{1 - D_R}{2}, \frac{1 + D_R}{2}\right), \tag{11}$$

$$(K_1, K_2) = \left(R_0\sqrt{A_R}, \frac{R_0}{\sqrt{A_R}}\right). \tag{12}$$

Analysis of evolutionary attractors

When mutation of the predators is taken into account in the model above, selection through population dynamics brings about their evolutionary dynamics. To analyse the qualitative features of the dynamics, we examine evolutionary attractors in the phenotype space $x = (\mu, \sigma)$, according to adaptive dynamics theory (Dieckmann and Law, 1996; Metz *et al.*, 1996; Geritz *et al.*, 1997), which is an extension of ESS theory. For analytical tractability, rare and small mutations and the existence of a stable equilibrium in population dynamics are assumed (see Metz *et al.*, 1996, for details). Although predator–prey systems can induce cyclic population dynamics, our system appears to have a global equilibrium as far as the dynamics was numerically simulated in the parameter regions used in this paper. Based on our assumptions, population dynamics is at equilibrium whenever a mutant emerges. Suppose a monomorphic population with phenotype x (called the *resident phenotype*) at equilibrium $\hat{n}(x)$ and a mutant $x' = (\mu', \sigma')$ that is slightly different from x. Whether the mutant can invade the population depends on *invasion fitness*, given by

$$s(x'; x) = \lim_{n(x')\to 0}\left[\frac{1}{n(x')}\cdot\frac{dn(x')}{dt}\right] = cM\int u(z, x')\cdot H(z)dz - d, \tag{13}$$

with $U(z) = M\int \hat{n}(x)u(z,\ x)dx$ and $R(z) = \hat{R}_1 r_1(z) + \hat{R}_2 r_2(z)$, where $\hat{R}_1$ and $\hat{R}_2$ are the equilibrium biomass of prey 1 and 2, respectively. Note that $s(x; x) = 0$ is always fulfilled for the population-dynamical equilibrium. If $s(x'; x) > 0$, the mutant can invade the resident population. If $s(x; x') < 0$ is also fulfilled, the mutant can replace the resident phenotype.

Since $|x' - x|$ is assumed to be very small, the sign of the mutant's fitness is given by the gradient of the invasion fitness ('fitness gradient'), $G(x) = (G_\mu(x), G_\sigma(x))$, where

$$G_\mu(x) = \left.\frac{\partial s(x'; x)}{\partial \mu'}\right|_{x'=x} = cM \int H(z) \frac{\partial u(z, x)}{\partial \mu} dz, \tag{14}$$

$$G_\sigma(x) = \left.\frac{\partial s(x'; x)}{\partial \sigma'}\right|_{x'=x} = cM \int H(z) \frac{\partial u(z, x)}{\partial \sigma} dz. \tag{15}$$

When $G(x)$ does not vanish, $s(x'; x) \simeq G(x)(x' - x)^T > 0$ gives $s(x; x') \simeq -G(x')(x' - x)^T < 0$. Thus as long as the gradient of invasion fitness does not vanish, trait substitution is repeated and the population evolves in the direction of the fitness gradient. This directional evolution continues until the population gets close to a point x^* where the fitness gradient vanishes ($G_\mu(x^*) = 0,\ G_\sigma(x^*) = 0$). Such a point is called the *evolutionarily singular point* (Metz *et al.*, 1996). An evolutionarily singular point is *strong convergence stable* (Leimar, 2005) – that is, an evolutionary attractor – if the first derivative of the fitness gradient vector, given by

$$C(x) = \begin{pmatrix} \dfrac{\partial G_\mu(x)}{\partial \mu} & \dfrac{\partial G_\mu(x)}{\partial \sigma} \\ \dfrac{\partial G_\sigma(x)}{\partial \mu} & \dfrac{\partial G_\sigma(x)}{\partial \sigma} \end{pmatrix}, \tag{16}$$

is negative definite at x^*.

A strong convergence stable point is locally evolutionarily stable if the second derivative of the invasion fitness vector ('fitness curvature' around a monomorphic population with phenotype x), given by a symmetric matrix,

$$D(x) = \begin{pmatrix} D_{\mu\mu}(x) & D_{\mu\sigma}(x) \\ D_{\sigma\mu}(x) & D_{\sigma\sigma}(x) \end{pmatrix} = \begin{pmatrix} \left.\dfrac{\partial^2 s(x'; x)}{\partial \mu'^2}\right|_{x'=x} & \left.\dfrac{\partial^2 s(x'; x)}{\partial \mu' \partial \sigma'}\right|_{x'=x} \\ \left.\dfrac{\partial^2 s(x'; x)}{\partial \mu' \partial \sigma'}\right|_{x'=x} & \left.\dfrac{\partial^2 s(x'; x)}{\partial \sigma'^2}\right|_{x'=x} \end{pmatrix}, \tag{17}$$

has negative eigenvalues, at x^* (Leimar, 2005). Conversely, if one (or both) of them is positive, the fitness landscape forms a saddle (or minima). The valley is steepest in the direction of the eigenvector with the maximum eigenvalue, which allows invasion into the resident x^* by a mutant x' that differs from x^* in direction (U. Dieckmann and J.A.J. Metz, in preparation). Moreover, the invading mutant can co-exist with the resident in a protected dimorphism when the evolutionarily unstable singular point is strongly convergence stable, which may result in *evolutionary branching* (Metz *et al.*, 1996; Geritz *et al.*, 1997; Dieckmann and Metz, in preparation). We call the maximum eigenvalue and the direction of its eigenvector the 'strength' and 'direction' of the disruptive selection, respectively.

In our model, the fitness gradients and curvatures are transformed into intuitively understandable shapes, by exploiting the condition $s(x; x) = 0$:

$$G_\mu(x) = \frac{d}{\sigma^2}\left[\int zE(z, x)dz - \mu\right] = \frac{d}{\sigma^2} m_1(x), \tag{18}$$

$$G_\sigma(x) = \frac{d}{\sigma^3}\left[\int (z-\mu)^2 E(z, x)dz - \sigma^2\right] = \frac{d}{\sigma^3} m_2(x), \tag{19}$$

$$D_{\mu\mu}(x) = \frac{d}{\sigma^4}\left[\int (z-\mu)^2 E(z, x)dz - \sigma^2\right] = \frac{d}{\sigma^4} m_2(x) = \frac{d}{\sigma} G_\sigma(x), \tag{20}$$

$$D_{\mu\sigma}(x) = \frac{d}{\sigma^5}\left[\int (z-\mu)^3 E(z, x)dz - 3\sigma^2 m_1(x)\right] = \frac{d}{\sigma^5} m_3(x) - 3\sigma G_\mu(x), \tag{21}$$

$$D_{\sigma\sigma}(x) = \frac{d}{\sigma^6}\left[\int (z-\mu)^4 E(z, x)dz - 3\sigma^4 - \sigma^2 m_2(x)\right] = \frac{d}{\sigma^6} m_4(x) - \sigma G_\sigma(x), \tag{22}$$

where

$$E(z, x) = \frac{cM}{d} \cdot u(z, x)H(z) \tag{23}$$

and

$$m_k(x) = \int (z-\mu)^k E(z, x)dz - \int (z-\mu)^k u(z, x)dz. \tag{24}$$

Since $s(x; x) = 0$ gives $\int E(z, x)dz = 1$, $E(z, x)$ can be translated as the 'effective resource pattern' for the utilization pattern $u(z, x)$. The function $m_k(x)$ is the k-th relative moment of the effective resource pattern to the utilization pattern. As for directional evolution, if the weighted average (first moment) of $E(z, x)$ is different from the mean of the utilization pattern (μ), then $G_\mu(x)$ favours evolutionary shift of μ towards the weighted average of $E(z, x)$. On the other hand, if the variance (second moment) of $E(z, x)$ is larger than the variance of the utilization pattern (σ^2), then $G_\sigma(x)$ favours the wider utilization pattern. Directional evolution halts when the first and second moments of $E(z, x)$ become the same as those of the utilization pattern, respectively. Note that $D_{\mu\mu}(x)$ is always proportional to $G_\sigma(x)$. Thus, at a singular point x^*, which fulfils $m_1(x^*) = m_2(x^*) = 0$ (i.e. $G_\mu(x^*) = 0$ and $G_\sigma(x^*) = 0$), the curvature of the fitness landscape is given by

$$D(x^*) = \frac{d}{\sigma^6}\begin{pmatrix} 0 & \sigma m_3(x^*) \\ \sigma m_3(x^*) & m_4(x^*) \end{pmatrix}. \tag{25}$$

Its maximum eigenvalue is

$$\lambda_0 = \frac{m_4(x^*) + \sqrt{m_4(x^*)^2 + 4\sigma^2[m_3(x^*)]^2}}{2} \tag{26}$$

Note that λ_0 is positive unless both $m_3(x^*) = 0$ and $m_4(x^*) < 0$ are fulfilled, which gives $\lambda_0 = 0$. In general, $m_3(x^*)$ is non-zero because the system has no force that favours $m_3(x^*) = 0$. Thus disruptive selection always exists at x^*, except for the special case. Since the eigenvector has a non-zero component in both the μ- and σ-directions in this case, it is expected that induced evolutionary branching always involves coupled diversification of μ and σ.

As for convergence stability, it was not obtained in an intuitive form. Instead, we examined evolutionarily singular points numerically, for various differences in quality, $D_R = |y_1 - y_2|$, and quantity, $A_R = K_1/K_2$, between the two resources. The number of strong convergence stable points in the phenotype space varies from 1 to 3 (Fig. 1a–d), along with

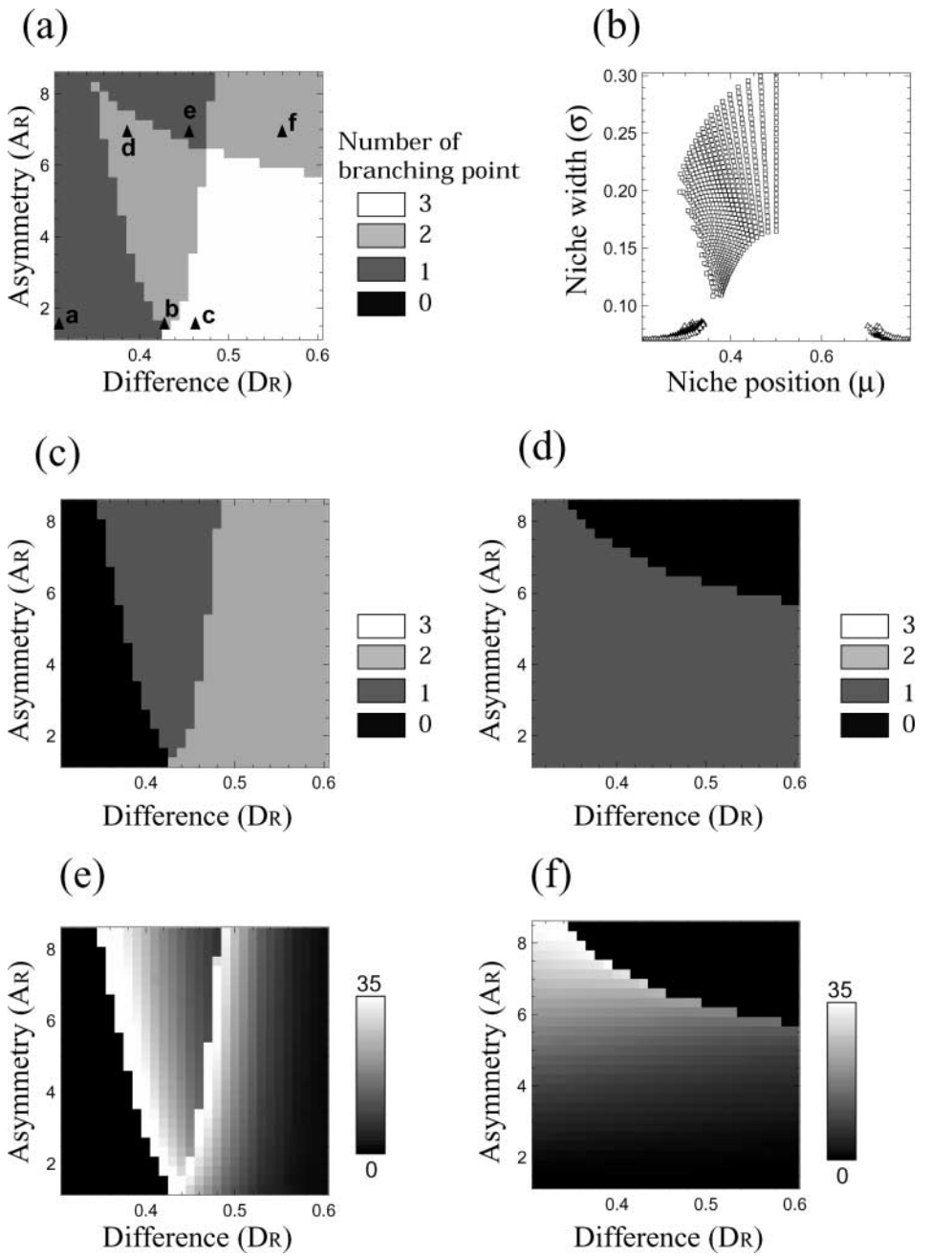

Fig. 1. Numbers of evolutionary branching points at various degrees of difference and biomass asymmetry between two resources. (a) Numbers of branching points. (b) Scatter plot of positions of branching points. (c) and (e) Numbers of specialist branching points and strengths of their disruptive selection, respectively. (d) and (f) Numbers of generalist branching points and strengths of their disruptive selection, respectively. Model parameters: $M = 30$, $R_0 = 400$, $\sigma_R = 0.07$, $d = 0.2$, $c = 0.1$, $\beta = \beta' = 1$, $\gamma = 2$.

D_R and A_R. As expected, all convergence stable points found were evolutionary branching points, except for symmetric resource distributions ($A_R = 1$) that give $m_3(x^*) = 0$ and $m_4(x^*) < 0$. Disruptive selection at all of the branching points favours coupled diversification of μ and σ.

The positions of these branching points form three clusters in the phenotype space (Fig. 1b). One cluster is located around the centre between the resources in niche position, and has large niche widths, which corresponds to generalists utilizing both resources with wide niches ('generalist branching points') (Fig. 2a–d). In contrast, the others have small niche widths, which correspond to specialists that mainly utilize one or other of the resources ('specialist branching points') (Fig. 2b–f). Specialist branching points exist when the distance between the resources is sufficiently large, while generalist branching points exist when the resource distance and the resource asymmetry are small. However, small resource asymmetry results in small $|D_{\mu\sigma}(x^*)|$ according to equation (25). In addition, a wide utilization pattern of the generalist covering both resources gives a bimodal shape of the effective resource distribution, which usually results in negative $m_4(x^*)$. In this case, $D_{\sigma\sigma}(x)$ is expected to be negative. As a consequence, the more symmetric the resource distribution becomes, the weaker the strength of disruptive selection at a generalist branching point (Fig. 2f). A generalist branching point and specialist branching points can co-exist depending on the shape of the resource distribution (Fig. 2b–d). This means that the evolutionary dynamics can be qualitatively different depending on the initial condition of the population.

It is notable that the internal of $H(z)$ does not appear in the above analyses. This allows us to examine the condition for evolutionary branching for other resource distributions with different definitions of their shape and growth, in the same manner as for the relative moments. That no evolutionarily singular point is evolutionarily stable holds for any resource distribution. In addition, a strong correlation between $D_{\mu\mu}(x)$ and $G_\sigma(x)$ is still expected even if the utilization pattern is not defined with a Gaussian function, as long as its deviation from the Gaussian function is small (Appendix 1).

EVOLUTIONARY DYNAMICS

To examine the expectations above, the evolutionary dynamics was calculated using two different methods.

Calculation methods

The first method we use to investigate the dynamics of evolution is based on the canonical equation (Dieckmann and Law, 1996), which can calculate directional evolution of a monomorphic population until it converges to a branching point and the co-evolution of the two populations after branching. Assuming independent but identical mutation processes for μ and σ, directional evolution of the niche position and width of a population with phenotype x is given by

$$\begin{pmatrix} \frac{d\mu}{dt} \\ \frac{d\sigma}{dt} \end{pmatrix} = \frac{\eta V \hat{n}(x)}{2} \begin{pmatrix} G_\mu(x) \\ G_\sigma(x) \end{pmatrix}, \tag{27}$$

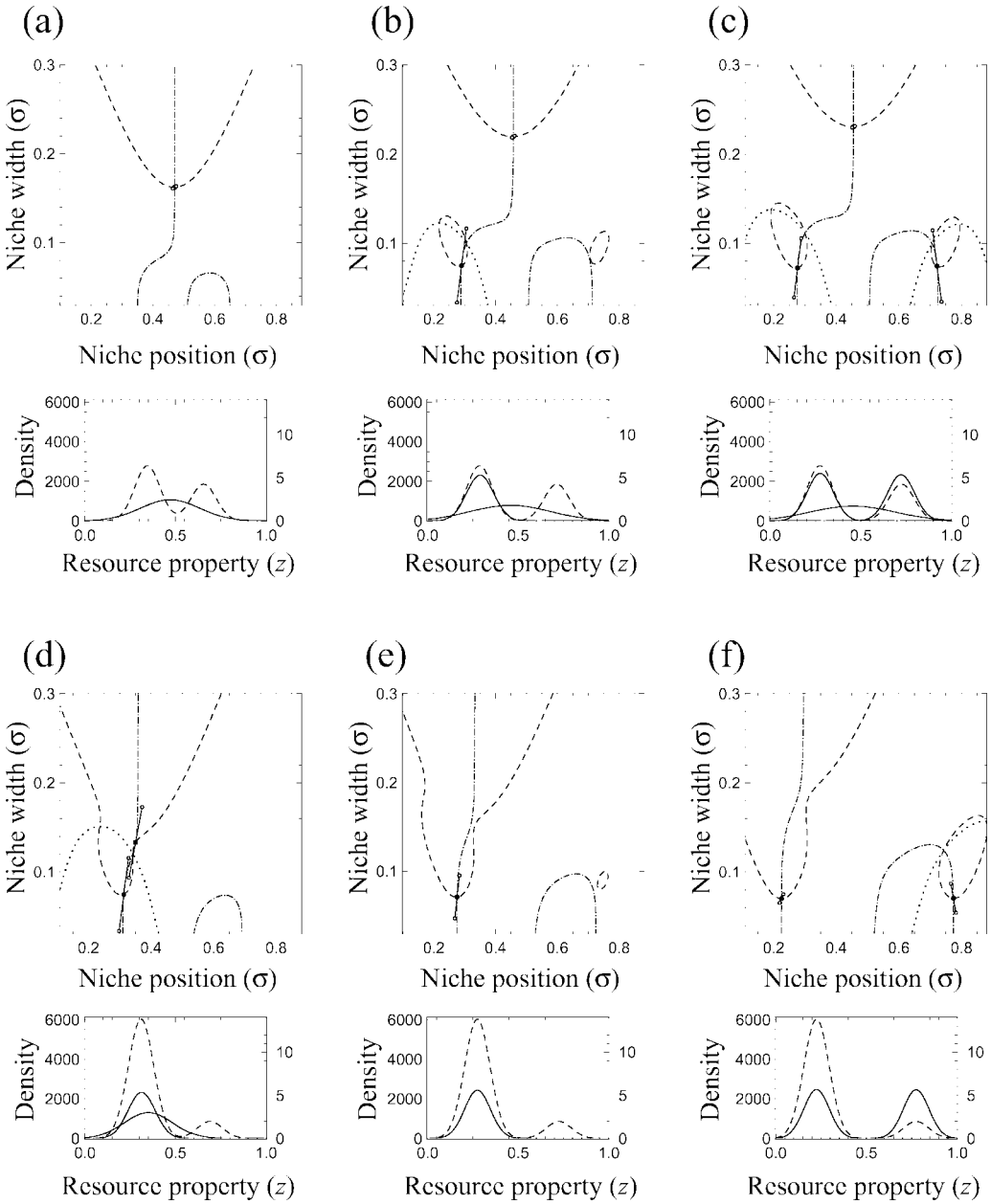

Fig. 2. Evolutionary branching points in the phenotype space and corresponding utilization patterns. The parameter values used for panels (a)–(f) correspond to the points indicated in Fig. 1a. In phenotype spaces, broken and dash-dotted lines indicate evolutionary null-isocline of μ and σ, respectively. Black dots indicate branching points, and the direction and strength of the disruptive selection are expressed by the length and direction of black line segments with appropriate linear scaling. Dotted lines are separatrixes among basins of branching points. In resource space (the smaller boxes), resource distributions at equilibrium without consumption are plotted with a dashed line on the left axis, while utilization patterns that correspond to the branching points in phenotype space are plotted with a solid line on the right axis.

where η is the mutation rate and V is the mutational variance, assuming it is equal for μ and σ (see Dieckmann and Law, 1996, for details). When the population converges to the branching point, it splits into two populations with slightly different phenotypes in the direction of the disruptive selection. Thus the whole process of evolutionary dynamics is governed by selection pressures.

To investigate the robustness of the predicted dynamics, we also used an individual-based simulation model. Individuals have traits μ and σ as quantitative traits based on multiple loci. In each time step Δt, individual i grows its biomass n_i by

$$\Delta n_i = \Delta t \cdot c \cdot n_i \int Mu(z, \mu_i, \sigma_i)H(z)dz, \tag{28}$$

whereas it dies with probability $d \cdot \Delta t$, so that the expected biomass change is concordant with equation (1).

After the resource competition and death phases, they reproduce offspring through mating. Mating probability between individual i and j is a decreasing function along with phenotypic distance, given by

$$P_m(i, j) = \exp\left(\frac{-(\mu_i - \mu_j)^2}{2\alpha_\mu^2}\right) \cdot \exp\left(\frac{-(\sigma_i - \sigma_j)^2}{2\alpha_\sigma^2}\right). \tag{29}$$

Here α_μ and α_σ determine how steeply the probability decreases with phenotypic distance in μ and σ, respectively. Such a direct link between ecological traits and mating probability exists in various populations and is thought to have an important role in their speciation processes (Rice and Salt, 1990; Schluter and Nagel, 1995; Feder, 1998). Successful matings produce offspring through gene recombination and mutation. Detailed procedures are explained in Appendix 2. [It would also be ecologically plausible to assume that the mating probability function depends on other traits instead of μ and σ (Dieckmann and Doebeli, 1999). Although we do not consider it for simplicity, this alternative should be explored.]

Calculated dynamics

Evolutionary dynamics calculated with the canonical equation coincided with expectations from analyses on branching points, in both the position and direction of evolutionary branching. In the case of the individual-based model, the position and direction were well predicted, as long as α_μ and α_μ were sufficiently small ($\alpha_\mu < 0.05$, $\alpha_\sigma < 0.05$) and equal to each other. With a large difference between the two parameters, the trait with smaller α tended to have a larger component in the direction of branching than expected.

Figures 3, 4, and 5 show typical pathways of evolutionary dynamics, when the phenotype space has one generalist branching point and two specialist branching points as in Fig. 2c. Figures 3a–c and Fig. 4 show evolutionary dynamics of a population that initially has a narrow niche width. The population first converges to one of the specialist branching points, S_1, where it specializes on resource 1 (Fig. 4d), and diversifies into two populations (Fig. 4e). One of the populations rapidly becomes a generalist and starts to utilize resource 2 with its wide niche (Fig. 4f), while the other population continues to utilize resource 1, slightly narrowing its niche under competitive pressure by the generalist population. When the niche position of the generalist population shifts sufficiently towards resource 2, it starts to specialize on that resource and eventually becomes a specialist (Fig. 4g). If a population specialized on resource 1 cannot change niche width, the fitness valley between the two

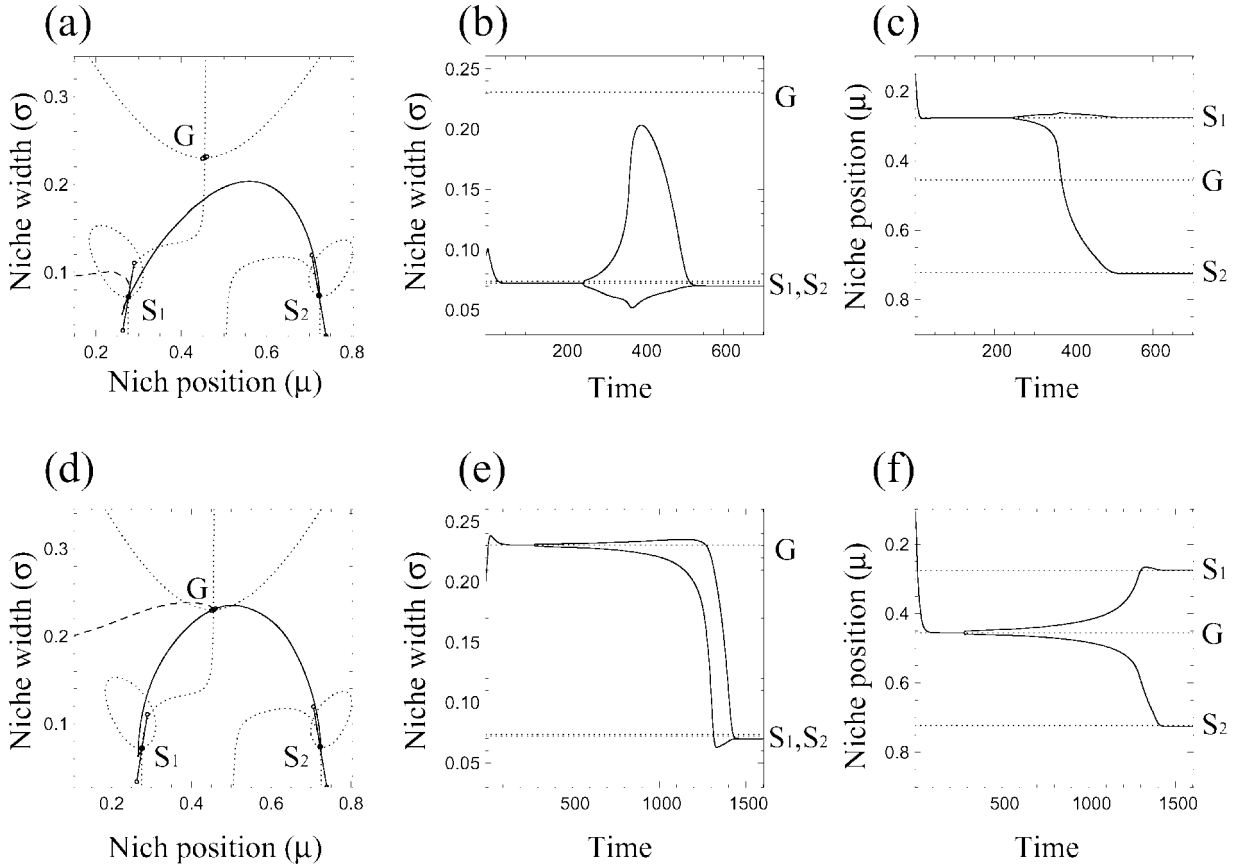

Fig. 3. Two different evolutionary scenarios of deterministic evolutionary dynamics by selection pressures. Evolutionary pathways started from phenotype $(\mu, \sigma) = (0.1, 0.1)$ and from phenotype $(\mu, \sigma) = (0.1, 0.2)$ are plotted in (a–c) and (d–f), respectively. Broken and solid lines in (a) and (c) indicate evolutionary pathways before and after evolutionary branching, respectively. Model parameters: $D_R = 0.45$, $A_R = 1.5$, and the others have the same values as in Fig. 1.

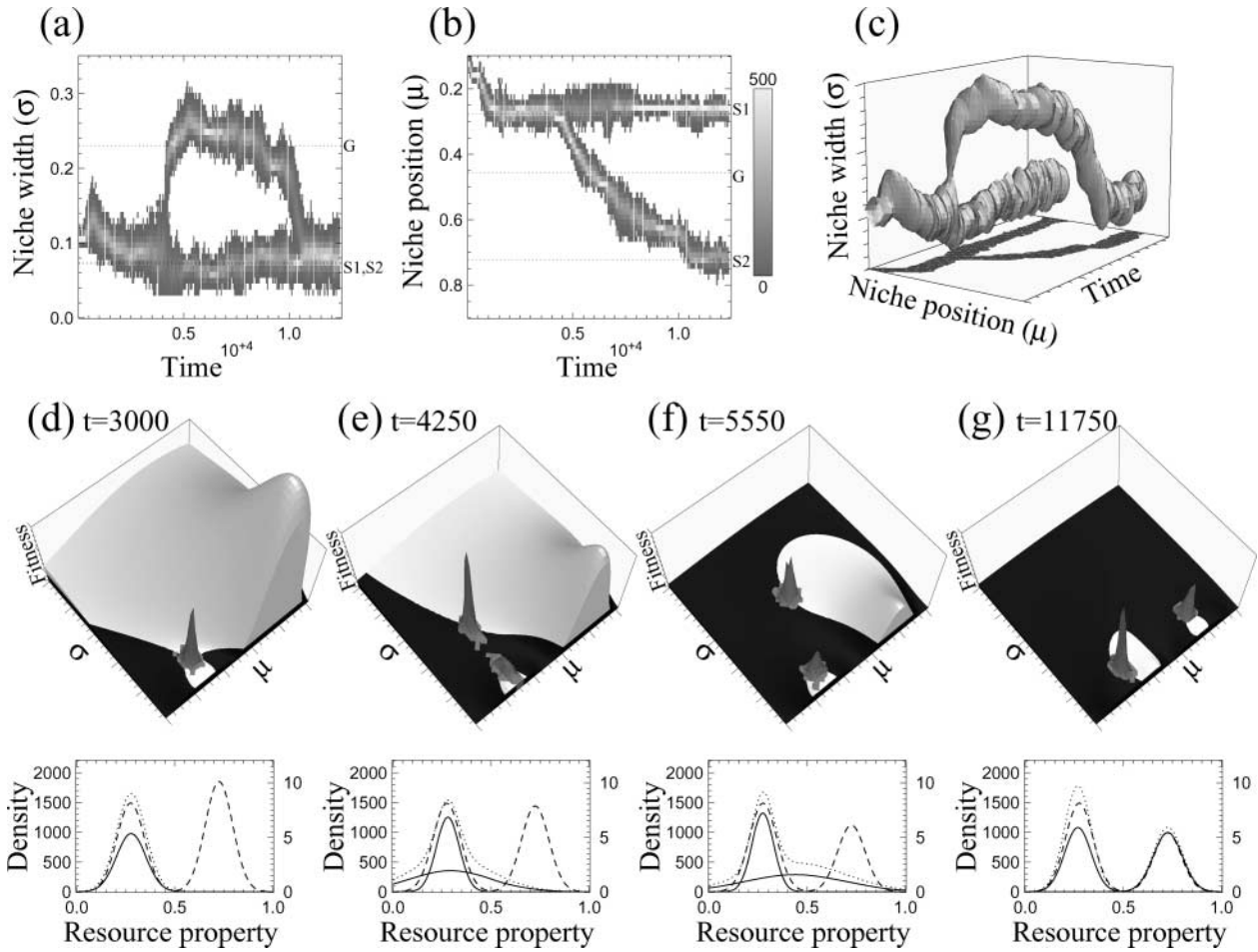
(a)
Niche width (σ)
0.0
0.1
0.2
0.3
G
S1,S2
0.5
1.0
10+4
Time
(b)
Niche position (μ)
0.2
0.4
0.6
0.8
S1
G
S2
500
0
0.5
1.0
10+4
Time
(c)
Niche width (σ)
Niche position (μ)
Time
(d) t=3000
(e) t=4250
(f) t=5550
(g) t=11750
Fitness
σ
μ
Density
2000
1500
1000
500
0
10
5
0
0.0
0.5
1.0
Resource property

resources can inhibit a niche shift towards resource 2 (Fig. 4d). Thus evolutionary niche generalization followed by specialization to get around the valley is favoured by selection.

In contrast, the evolutionary dynamics of a population that initially has a wide niche width, calculated with the canonical equation, is shown in Figs. 3d–f. In this case, the population first converges to the generalist branching point *G*, where it utilizes both resources with its wide niche, and diversifies into two subpopulations each of which gradually specializes on one or other resource. Since disruptive selection at the generalist branching point is weak in this case as explained, this branching point leads to a slower branching process than a specialist branching point. In the case of the individual-based model, evolutionary branching is not likely to occur with this weak disruptive selection, because gene recombination through mating counteracts the disruptive selection. However, sufficiently large mutation rates and/or small mating ranges favour evolutionary branching (Fig. 5).

It is notable that evolutionary dynamics through a specialist branching point has evolutionary branching first, followed by niche expansion of one of the split populations with niche generalization and specialization, while evolutionary dynamics through a generalist branching point has generalization first, followed by evolutionary branching and specialization of the split populations. The final evolutionary outcome is the same, but the order of these processes is different. If both types of branching points exist in the phenotype space, which order of dynamics arises depends on the initial phenotype of the population, as shown here.

DISCUSSION

The role of niche width evolution in evolutionary branching

Our analysis of evolutionary attractors intuitively shows relationships among directional and disruptive selection in niche position and width, as relations among the relative statistical moments of the effective resource pattern to the utilization pattern. An important result is that almost all convergence stable points are evolutionary branching points.

In a previous model on evolution of niche position with fixed niche width under a unimodal resource distribution (Dieckmann and Doebeli, 1999), evolutionary branching occurred only if the niche width was narrower than the resource distribution. Assuming a fixed niche width in our model provides an identical condition: the variance of the utilization pattern is smaller than that of the effective resource pattern, i.e. $m_2(x^*) > 0$.

Fig. 4. Evolutionary dynamics through a specialist branching point based on individual-level stochastic processes. Time evolution of the phenotype distribution is projected on the time-σ surface (a) and the time-μ space (b), and represented as an isosurface at two individuals with smoothing (c). (d–i) show states in phenotype and resource space at different time steps. In phenotype space, phenotype distributions (grey polygons) and fitness landscapes (i.e. invasion fitness) above 0 (light-grey surface) and below 0 (black surface) are represented. In resource space, average utilization patterns of isolated populations (solid line) are plotted on the right axis, while the resource distribution (broken line) and the total utilization distribution (dash-dotted line) are plotted on the left axis. Model parameters: $k_0 = 50$, $k_1 = 100$, $\alpha_\mu = 4 \times 10^{-2}$, $\alpha_\sigma = 3 \times 10^{-2}$, $b = 0.4$, $\eta_\mu = 2 \times 10^{-5}$, $\eta_\sigma = 6 \times 10^{-5}$, $L_\mu = L_\sigma = 30$, the initial phenotype $(\mu, \sigma) = (0.13, 0.092)$, and the others have the same values as in Fig. 2.

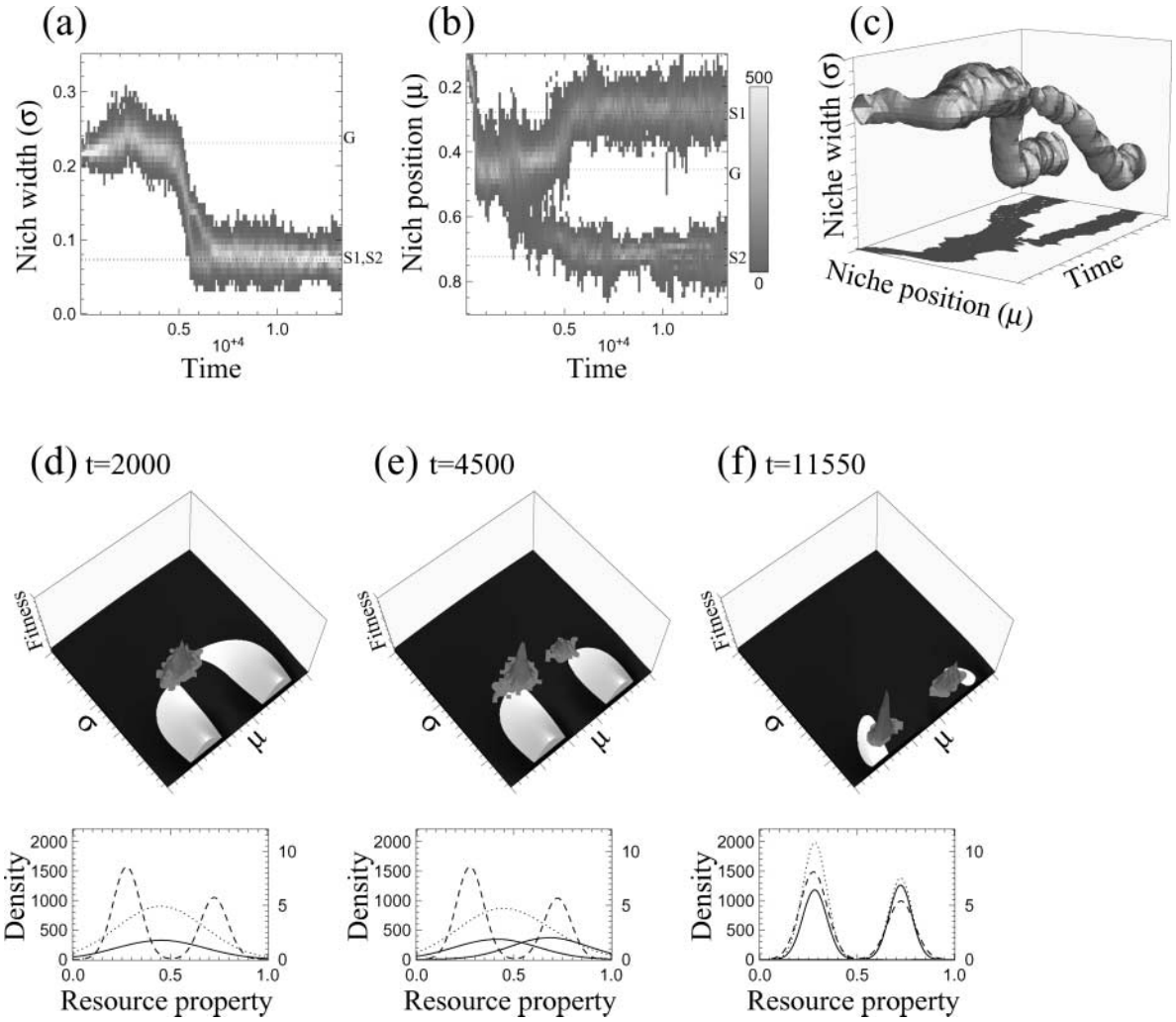
(a)
Nich width (σ)
0.3
0.2
0.1
0.0
G
S1,S2
0.5
1.0
10^+4
Time
(b)
Nich position (μ)
0.2
0.4
0.6
0.8
S1
G
S2
500
0
0.5
1.0
10^+4
Time
(c)
Niche width (σ)
Niche position (μ)
Time
(d) t=2000
(e) t=4500
(f) t=11550
Fitness
σ
μ
Density
2000
1500
1000
500
0
10
5
0
0.0
0.5
1.0
Resource property

The evolution of niche width is viewed as suppressing the diversification of niche position (Ackermann and Doebeli, 2004). Although their model differs from ours in its functional response and in the growth function for the resource distribution, our results also show that diversification only in niche position that requires $m_2(x^*) > 0$ is suppressed by directional evolution of niche width that leads to $m_2(x^*) = 0$. If the resource distribution as well as the utilization pattern is a unimodal Gaussian distribution ($D_R = 0$), which corresponds to the situation studied by Ackermann and Doebeli (2004), the effective resource pattern becomes proportional to the utilization pattern when a monomorphic population is located at the evolutionarily singular point. In this case, the third and fourth relative moments, $m_3(x^*)$ and $m_4(x^*)$, are also zero. Thus evolutionary branching is not expected in this case, in line with Ackermann and Doebeli (2004).

However, it would be ecologically more plausible to assume that the shape of the effective resource pattern and that of the utilization pattern are not exactly the same even if their first and second moments are the same. In such a situation, $m_3(x^*)$ is expected to be non-zero, which always favours evolutionary branching through coupled diversification of niche position and width. In addition, if $m_4(x^*) > 0$, evolutionary branching in niche width only is also possible. The model of Ackermann and Doebeli (2004) seems to have such branchings also, if an asymmetric or multi-modal resource distribution is assumed. It can be said that evolution of niche width enhances evolutionary branching by providing other ways of diversification while suppressing diversification in niche position only.

Another novel feature of our results is two types of evolutionary branching points for different orders of evolutionary processes: generalist branching points and specialist branching points. The dynamics associated with a generalist branching point – that is, niche generalization followed by evolutionary branching and specialization – coincides with the evolutionary dynamics in Egas *et al.* (2005). Thus evolutionary branching points found in their model seem to correspond to generalist branching points in our model. While Egas *et al.* (2005) considered behavioural changes of foraging strategies and sub-optimal foraging behaviour is required for the branching, such changes in strategies are not considered in our model. Thus the effect of sub-optimal foraging behaviour may also be translated into the relationship between the effective resource and utilization patterns in our model.

On the other hand, specialist branching points that induce evolutionary branching of a specialist population followed by significant niche generalization and specialization of one of the split populations shifting the new resource, might be a new type of branching point. This branching point seems to correspond to one of the two branching points found in Meszena *et al.* (1997), who studied the evolution of niche position with fixed width, under the existence of two types of resources. One branching point is close to an optimal niche position in either of two resources, which corresponds to the specialist branching point in our model. The other branching point is between the optimal niche positions, which corresponds to the generalist branching point in our model. However, the two types of branching point cannot exist simultaneously in their model. Co-existence is also not possible in our model if niche width is fixed. Thus evolution of niche width is the key factor

Fig. 5. Evolutionary dynamics through a generalist branching point based on individual-level stochastic processes. Time evolution of the phenotype distribution (a–c), and states in phenotype and resource space (d–f), are plotted in the same way as in Fig. 4. Model parameters: the initial phenotype $(\mu, \sigma) = (0.13, 0.21)$, $\eta_\mu = 6 \times 10^{-5}$ only for (c–j), and the others have the same values as in Fig. 4.

for co-existence. In addition, a generalist convergence stable point is always a branching point in our model, while in their model it becomes evolutionarily stable when the difference between the two resources is small. This is another effect of the evolution of niche width.

The next step in the analysis would be convergence stability. Since almost all convergence stable points are branching points in our model, convergence stability of evolutionarily singular points is important to characterize possible evolutionary dynamics. Although this is not obtained intuitively in our model, a different formulation of the functional response enables convergence stability to be expressed, as well as the other conditions for evolutionary branching, with the relative moments. This helps us to understand how the number and kind of branching points change with D_R and A_R (H. Ito, in preparation).

Costs for evolution of niche width

Our model assumes that the total amount of utilization is constant, irrespective of its position and width. However, there may be some costs for niche specialization or generalization in real organisms. If a cost for generalization exists in our model, an evolutionary singular point x^* shifts towards a narrower niche than that of the effective resource pattern (i.e. $m_2(x^*) > 0$ when $G_\sigma(x^* = 0)$. This results in positive $D_{\mu\mu}(x^*) = m_2(x^*)$, which can induce evolutionary branching in niche position at least, as in Ackermann and Doebeli (2004). Conversely, a cost for specialization results in negative $D_{\mu\mu}(x^*)$ and suppresses diversification of niche position, as in Ackermann and Doebeli (2004). Even in this case, sufficiently large $m_3(x^*)$ or $m_4(x^*)$ allows evolutionary branching. Since $m_3(x^*)$ is not usually zero in both cases above, the resulting evolutionary branching is expected to lead to diversification of both niche width and position.

The direction of evolutionary branching in sexual populations

In our simulations in the two-dimensional phenotype space for sexual populations, the strength of assortative mating affected not only the likelihood of evolutionary branching but also its direction, through differences in the strength of assortative mating among the traits. The direction of branching is tilted towards the trait with stronger assortativeness. This is likely due to the fact that disruptive selection can counteract recombination more easily when the mating range is smaller. It would be worth investigating how the strength of assortative mating affects evolutionary branching, in combination with local fitness landscapes and mutation supply.

Comparison with empirical studies

Our results suggest that real populations have experienced specialist–generalist evolutionary dynamics with niche expansion and division of populations. Although we do not know of any single study covering the whole evolutionary dynamics demonstrated here (niche generalization, division, and specialization), each component of the dynamics is supported by corresponding empirical studies. For speciation with niche division through resource competition, there is substantial empirical support (Schluter, 2000), including cichlid fish (Schliewen *et al.*, 1994), stickleback (Schluter and Nagel, 1995), apple maggot fly (Feder *et al.*, 1997), and aphids (Caillaud and Via, 2000). These studies report niche differentiation in host-plant (aphids and apple maggot fly), as well as in diet (cichlid fish and stickleback), through resource

competition. As for the evolutionary dynamics of niche width, a combination of phylogenetic and ecological approaches has given histories of niche specialization as well as generalization through repeated evolutionary branching in many species groups. Strong support comes from studies on phytophagous insects [bark beetles (Kelley and Farrell, 1998), butterflies (Janz et al., 2001), walking sticks (Crespi and Sandoval, 2000), and vines (Armbruster and Baldwin, 1998)] that show the evolutionary dynamics of host-plant ranges.

ACKNOWLEDGEMENTS

We thank Eva Kisdi for her thoughtful advice and encouragement. We also thank Ulf Dieckmann and Michael Doebeli for valuable comments. H.I. thanks David Munro for inventing Yorick, a free tool for numerical analysis and visualization with great performance and flexibility. All figures in this paper were made with Yorick. H.I. was supported by a Research Fellowship of the Japan Society for the Promotion of Science for Young Scientists.

REFERENCES

Abrams, P.A. and Ginzburg, L.R. 2000. The nature of predation: prey dependent, ratio dependent, or neither? *Trends Ecol. Evol.*, **15**: 337–341.

Ackermann, M. and Doebeli, M. 2004. Evolution of niche width and adaptive diversification. *Evolution*, **58**: 2599–2612.

Arditi, R. and Ginzburg, L.R. 1989. Coupling in predator–prey dynamics: ratio-dependence. *J. Theor. Biol.*, **139**: 311–326.

Armbruster, W.S. and Baldwin, B.C. 1998. Switch from specialized to generalized pollination. *Nature*, **394**: 632.

Beddington, J.R. 1975. Mutual interference between parasites or predators and its effects on searching efficiency. *J. Anim. Ecol.*, **44**: 331–340.

Caillaud, M. and Via, S. 2000. Specialized feeding behavior influences both ecological specialization and assortative mating in sympatric host races of pea aphids. *Am. Nat.*, **156**: 606–621.

Crespi, J.B. and Sandoval, C.P. 2000. Phylogenetic evidence for the evolution of ecological specialization in *Timema* walking-sticks. *J. Evol. Biol.*, **13**: 249–262.

DeAngelis, D.L., Goldstein, R.A. and O'Neill, R.V. 1975. A model for trophic interactions. *Ecology*, **56**: 881–892.

Dieckmann, U. and Doebeli, M. 1999. On the origin of species by sympatric speciation. *Nature*, **400**: 354–357.

Dieckmann, U. and Law, R. 1996. The dynamical theory of coevolution: a derivation from stochastic ecological processes. *J. Math. Biol.*, **34**: 579–612.

Di-Giulio, M. 2001. The universal ancestor was a thermophile or a hyperthermophile. *Gene*, **281**: 11–17.

Doebeli, M. and Dieckmann, U. 2000. Evolutionary branching and sympatric speciation caused by different types of ecological interactions. *Am. Nat.*, **156**: s77–s101.

Egas, M., Sabelis, M.W. and Dieckmann, U. 2005. Evolution of specialization and ecological character displacement of herbivores along a gradient of plant quality. *Evolution*, **59**: 507–520.

Feder, J.L. 1998. The apple maggot fly, *Rhagoletis pomonella*: flies in the face of conventional wisdom about speciation? In *Endless Forms: Species and Speciation* (D.J. Howard and S.H. Berlocher, eds.), pp. 130–144. New York: Oxford University Press.

Feder, J.L., Roethele, J.B., Wlazlo, B. and Berlocher, S.H. 1997. Selective maintenance of allozyme differences among sympatric host races of the apple maggot fly. *Proc. Natl. Acad. Sci. USA*, **94**: 11417–11421.

Geritz, S.A.H., Metz, J.A.J., Kisdi, E. and Meszena, G. 1997. Dynamics of adaptation and evolutionary branching. *Phys. Rev. Lett.*, **78**: 2024–2027.

Geritz, S.A.H., Kisdi, E., Meszena, G. and Metz, J.A.J. 1998. Evolutionarily singular strategies and the adaptive growth and branching of the evolutionary tree. *Evol. Ecol.*, **12**: 35–57.

Janz, N., Nyblom, K. and Nylin, S. 2001. Evolutionary dynamics of host plant specialization: a case study of the tribe Nymphalini. *Evolution*, **55**: 783–796.

Kelley, S.T. and Farrell, B.D. 1998. Is specialization a dead end? The phylogeny of host use in dendroctonus bark beetles (Scolytidae). *Evolution*, **52**: 1731–1743.

Leimar, O. 2005. The evolution of phenotypic polymorphism: randomized strategies versus evolutionary branching. *Am. Nat.*, **165**: 669–681.

MacArthur, R. 1972. *Geographical Ecology*. New York: Harper & Row.

Meszena, G., Czibula, I. and Geritz., S.A.H. 1997. Adaptive dynamics in a 2-patch environment: a toy model for allopatric and parapatric speciation. *J. Biol. Syst.*, **5**: 265–284.

Metz, J.A.J., Geritz, S.A.H., Meszena, G., Jacobs, F.J.A. and van Heerwaarden, J.S. 1996. Adaptive dynamics: a geometrical study of the consequences of nearly faithful reproduction. In *Stochastic and Spatial Structures of Dynamical Systems* (S.J. van Strien and S.M. Verduyn Lunel, eds.), pp. 83–231. Amsterdam: North-Holland.

Pianka, E.R. 1983. *Evolutionary Ecology*, 3rd edn. New York: Harper & Row.

Rice, W.R. and Salt, G. 1990. The evolution of reproductive isolation as a correlated character under sympatric conditions: experimental evidence. *Evolution*, **44**: 1140–1152.

Schilewen, U.K., Tautz, D. and Paabo, S. 1994. Sympatric speciation suggested by monophyly of crater lake cichlids. *Nature*, **368**: 629–632.

Schluter, D. 2000. Ecological character displacement in adaptive radiation. *Am. Nat.*, **156**: S4–S16.

Schluter, D. and Nagel, L. 1995. Parallel speciation by natural selection. *Am. Nat.*, **146**: 292–301.

APPENDIX 1

Here we examine the relationship between the fitness curvature in the position, and the fitness gradient in the width, of an arbitrary shape of utilization pattern $u(z)$ that fulfils $\int u(z)dz = 1$. First, we explain how a phenotype space appropriate for the analysis is defined for $u(z)$. The position μ and width σ of $u(z)$ are defined as the first and second moments of $u(z)$:

$$\mu = \int zu(z)dz, \tag{30}$$

$$\sigma = \int (z-\mu)^2 u(z)dz. \tag{31}$$

Then $u(z)$ is normalized by μ and σ,

$$u(z) = \frac{1}{\sigma}\upsilon\left(\frac{z-\mu}{\sigma}\right), \tag{32}$$

where information on $u(z)$ is decomposed into two valuables, μ and σ, and a shape function, $\upsilon(z)$, fulfilling $\upsilon_0 = \int \upsilon(z)dz = 1$, $\upsilon_1 = \int z\upsilon(z)dz = 0$, and $\upsilon_2 = \int z^2\upsilon(z)dz = 1$. Since substituting equation (32) into equations (30) and (31) gives identities, μ, σ, and $\upsilon(z)$ are independent of each other. For example, doubling μ changes only the position of $u(z)$ into 2μ, while doubling σ expands $u(z)$ along the z-axis by two times and reduces its height by half without any change of μ and $\upsilon(z)$. As for higher moments of $\upsilon(z)$, we denote the k-th moment of $\upsilon(z)$ with υ_k, that is,

$$\upsilon_k = \int z^k \upsilon(z)dz. \tag{33}$$

Then, any possible utilization pattern is represented with a vector with infinite dimension, $x = (\mu, \sigma, \upsilon_3, \upsilon_4, \ldots)$. We treat this as a phenotype space for $u(z)$ and re-denote it with $u(z, x)$. Note that not only μ but also σ can be changed independently of the other traits, which allows us to obtain fitness gradients and curvatures in μ and σ. Any mutational change of $u(z)$ can be decomposed into combinations of changes of these traits.

Suppose an arbitrary community represented by a phenotype distribution $\hat{n}(x)$ at population-dynamical equilibrium, which gives the corresponding $H(z)$ according to equations (7) and (8) in the main text. Here we assume that the community has a monomorphic population with phenotype $x = (\mu, \sigma, \upsilon_3, \upsilon_4, \ldots)$, and examine the local shape of fitness landscape around it. Considering the Taylor expansion of $H(z)$ at $z = \mu$,

$$H(z) = \sum_{k=0}^{\infty} \frac{1}{k!} \frac{d^k H(z)}{dz^k}\bigg|_{z=\mu} (z-\mu)^k = \sum_{k=0}^{\infty} a_k (z-\mu)^k, \tag{34}$$

where $a_k = \frac{1}{k!} \frac{d^k H(z)}{dz^k}\Big|_{z=\mu}$, we expand the fitness function as

$$\frac{1}{n(x)} \frac{dn(x)}{dt} = cM \int u(z, x) H(z) dz - d$$

$$= cM \sum_{k=0}^{\infty} a_k \int (z-\mu)^k u(z, x) dz - d. \tag{35}$$

We assume $cM = 1$ without loss of generality. Suppose a mutant phenotype $x' = (\mu', \sigma', \upsilon_3', \upsilon_4', \ldots)$ that slightly differs from x. With the following relationships,

$$(z-\mu)^k = [(z-\mu') + (\mu'-\mu)]^k = \sum_{k=0}^{k} \binom{k}{l} (\mu'-\mu)^l (z-\mu')^{k-l},$$

$$\int (z-\mu')^{k-l} u(z, x') dz = \sigma'^{k-l} \upsilon'_{k-l}, \tag{36}$$

the invasion fitness of x' is expanded as

$$\int u(z, x') H(z) dz - d = -d + \sum_{k=0}^{\infty} a_k \sum_{l=0}^{k} \binom{k}{l} (\mu'-\mu)^l \int (z-\mu')^{k-l} u(z, x') dz$$

$$= -d + a_0 + a_1 \mu' + a_2 [\sigma'^2 + (\mu'-\mu)^2] \tag{37}$$

$$+ \sum_{k=3}^{\infty} \left(\sigma'^k \upsilon'_k + k(\mu'-\mu) \sigma'^{k-1} \upsilon'_{k-1} + \frac{k(k-1)}{2} (\mu'-\mu)^2 \sigma'^{k-2} \upsilon'_{k-2} + (\mu'-\mu)^3 q_k(x') \right).$$

The $q_k(x')$ is a polynomial composed of μ', σ', υ'_3, υ'_4, . . . Then the fitness curvature in μ is expanded as

$$D_{\mu\mu}(x) = \left[\frac{\partial^2}{\partial \mu'^2} \int u(z, x') H(z) dz \right]_{x'=x}$$

$$= 2a_2 + \sum_{k=3}^{\infty} a_k \left[k(k-1) \sigma'^{k-2} \upsilon'_{k-2} \right.$$

$$\left. + (\mu' - \mu) \left\{ 6q_k(x') + 6(\mu' - \mu) \frac{\partial q_k(x')}{\partial \mu'} + (\mu' - \mu)^2 \frac{\partial^2 q_k(x')}{\partial \mu'^2} \right\} \right]_{x'=x}. \quad (38)$$

Here the term multiplied by $(\mu' - \mu)$ becomes zero after exploiting $x' = x$, which yields

$$D_{\mu\mu}(x) = 2a_2 + \sum_{k=3}^{\infty} k(k-1) a_k \sigma^{k-2} \upsilon_{k-2}. \quad (39)$$

Similarly, the fitness gradient in σ is expanded as

$$G_\sigma(x) = \left[\frac{\partial}{\partial \sigma'} \int H(z) u(z, x') dz \right]_{x'=x}$$

$$= 2a_2\sigma + \sum_{k=3}^{\infty} a_k \left[k\sigma'^{k-1} \upsilon'_k + k(k-1)(\mu' - \mu)\sigma'^{k-2} \upsilon'_{k-1} \right.$$

$$\left. + \frac{k(k-1)(k-2)}{2} (\mu' - \mu)^2 \sigma'^{k-3} \upsilon'_{k-2} + (\mu' - \mu)^3 \frac{\partial q_k(x')}{\partial \sigma'} \right]_{x'=x}$$

$$= 2a_2\sigma + \sum_{k=3}^{\infty} k a_k \sigma^{k-1} \upsilon_k. \quad (40)$$

Next, we compare equations (39) and (40). They are proportional when $u(z, x)$ is a Gaussian distribution, according to the main text. Thus we consider 'moment deviations' of $\upsilon(z)$ from the normalized Gaussian distribution, $\frac{1}{\sqrt{2\pi}} \exp\left(\frac{-z^2}{2}\right)$. The k-th moment deviation $\delta\upsilon_k$ is defined by

$$\delta\upsilon_k = \upsilon_k - \omega_k, \quad (41)$$

where

$$\omega_k = \int z^k \frac{1}{\sqrt{2\pi}} \exp\left(\frac{-z^2}{2}\right) = \begin{cases} 0 & \text{for odd } n \\ \prod_{l=1}^{k/2} (2l-1) & \text{for even } n \end{cases} \quad (42)$$

In this case, the following relationship is fulfilled for $k > 1$:

$$\omega_k = (k-1)\omega_{k-2}. \quad (43)$$

Substituting this into equations (39) and (40) yields

$$D_{\mu\mu}(x) = 2a_2 + \sum_{k=3}^{\infty} ka_k\sigma^{k-2}[(k-1)\omega_{k-2} + (k-1)\delta\upsilon_{k-2}], \tag{44}$$

$$\frac{1}{\sigma} G_\sigma(x) = 2a_2 + \sum_{k=3}^{\infty} ka_k\sigma^{k-2}[(k-1)\omega_{k-2} + \delta\upsilon_k]. \tag{45}$$

Clearly, when $\delta\upsilon_k \to 0$ for all k, the two equations become equal. If a_2 (i.e. the curvature of $H(z)$ around μ) is not small and if $\delta\upsilon_k/\omega_k$ for any k (≥ 3) is small, their strong positive correlation is expected.

When the deviations are large, on the other hand, the relationship is more dependent on the local shape of $H(z)$ around $\mu - 2\sigma < z < \mu + 2\sigma$. To see how the deviations change the situation at an evolutionarily singular point, we assume that all a_k for $k > 5$ are very small (i.e. $H(z)$ has less than three peaks around $\mu \pm 2\sigma$). Subtracting equation (45) from equation (44) gives

$$D_{\mu\mu}(x) = \frac{1}{\sigma} G_\sigma(x) + \sum_{k=3}^{\infty} ka_k\sigma^{k-2}\,[(k-1)\delta\upsilon_{k-2} - \delta\upsilon_k]$$

$$\simeq \frac{1}{\sigma} G_\sigma(x) - 3a_3\sigma\delta\upsilon_3 - 4a_4\sigma^2\delta\upsilon_4.$$

At an evolutionary singular point x^* (i.e. $G_\mu(x^*) = G_\sigma(x^*) = 0$), $D_{\mu\mu}(x^*)$ is negative if $3a_3\delta\upsilon_3 + 4\sigma a_4\delta\upsilon_4 > 0$. Since $a_3\delta\upsilon_3 > 0$ and $a_4\delta\upsilon_4 > 0$ mean similarity of $\mu(z, x)$ to $H(z)$ in terms of the third and forth moments, respectively, $D_{\mu\mu}(x^*)$ is expected to be negative if $\mu(z, x^*)$ is similar to $H(z)$ in skewness and kurtosis around μ. In such circumstances, evolutionary diversification in niche position only is suppressed. Conversely, if $\mu(z, x^*)$ differs from $H(z)$ in signs of both skewness and kurtosis around μ, evolutionary diversification in niche position only might be favoured.

APPENDIX 2

In our individual-based model, individuals are diploid, and have μ and σ as quantitative traits with L_μ and L_σ loci, respectively. The k-th locus for μ has two integers μ_{k0} and μ_{k1}, and the value of μ is given by $\Sigma_{k=1}^{L_\mu}(\mu_{k0} + \mu_{k1})/(2L_\mu)$. Similarly, the value of σ is given by $\Sigma_{k=1}^{L_\sigma}(\sigma_{k0} + \sigma_{k1})/(2L_\sigma)$.

Mating is expressed by repeating a 'unit process' by $B\cdot[k_0 + k_1\cdot B/(k_1 + B)]$ times, where $B = \Sigma_i\lfloor 2n_i/b\rfloor$, and b denotes a constant biomass for eggs. Thus there are $k_0 + k_1\cdot B/(k_1 + B)$ times of mating opportunities per individual. This is a combination of constant mating rate k_0 and type-II functional response with saturation constant k_1.

The unit process is as follows. First, individuals i and j are chosen with probabilities $\lfloor 2n_i/b\rfloor/B$ and $\lfloor 2n_j/b\rfloor/B$, respectively. Second, if the biomasses of both individuals are more than $b/2$, one individual with biomass b is produced at probability $P_m(i, j)$, subtracting $b/2$ from the biomasses of both parents. The production of an individual is operated by combining gametes from the two parents through free recombination (all loci are independent of each other) for its genome, and giving biomass b to it. Mutation occurs at each locus as a stepwise mutation (adding +1 or −1) at small probabilities η_μ and η_σ for μ and σ, respectively.